# Modelling the dynamics of fibropapilloma disease in the Hawaiian green sea turtle population

Milani Chaloupka

Ecological Modelling Services P/L
PO Box 6150, University of Queensland, St Lucia, Queensland, 4067, Australia

April 2015

**Prepared for the**
**Western Pacific Regional Fisheries Management Council**
**Honolulu, Hawaii, USA**

## Summary

We explored the impact of a major chronic disease (fibropapillomatosis, FP) on survival, recapture and disease transition probabilities in a green turtle population resident in waters around Molokai, Hawaii. We used a sizeclass-specific multistate capture-mark–recapture analysis of 1792 individually tagged turtles sampled over a 24-year period. Size classes comprised 2 groups: small (< 60 cm SCL) and large (≥ 60 cm SCL) immature turtles. Each turtle was assigned at each encounter to a particular FP disease state (disease-free, diseased with FP scores > 0) where the transition probabilities among states, conditional on apparent survival, are analogous to probabilities of new infection and recovery from infection. We then fitted a range of models using MARK with model selection based on the quasi-likelihood form of AIC corrected for overdispersion and sample size. We found that FP infection resulted in lower apparent survival for large diseased turtles but not so for small diseased turtles compared to disease-free turtles. The estimated annual survival probability for large diseased turtles was ca. 0.75 (95% CI: 0.64-0.83) and ca. 0.85 (95% CI: 0.80-0.89) for small or large disease-free turtles. Recapture probabilities were time-varying but were independent of either disease state or sizeclass suggesting no sampling bias or behavioral differences for the diseased turtles. The estimated disease state transition probabilities suggested a rapidly increasing infection rate following the disease outbreak in the early-1980s followed by a significant and gradual decline from the mid-1990s as the disease ran its course. This infection rate function reflected well the apparent FP disease prevalence curve estimated for this population. At the peak of the epidemic in the mid-1990s it was estimated that the infection probability was > 0.43 (95% CI: 0.29-0.58). The current annual infection rate has declined to ca. 0.032. The estimated annual disease recovery probabilities were not a function of time but might be sizeclass-specific with smaller turtles apparently recovering from the disease at a slightly higher probability ca. 0.18 (95% CI: 0.11-0.28) compared to larger turtles at ca. 0.13 (95% CI: 0.06-0.26). This is the first comprehensive study of the long-term dynamics of a chronic disease for a large marine species.

## Introduction

Reliable estimates of survival (mortality) and breeding probabilities are needed for modelling the risk for marine turtle exposure to various anthropogenic hazards (Chaloupka

2003, Bjorndal et al 2011). While estimates of cause-specific mortality for marine turtles can be derived from indirect sources such as strandings (Chaloupka et al 2008b) by far the most useful source is from a capture-mark-recapture program of either nesting turtle populations (Troëng & Chaloupka 2007) or foraging ground populations Chaloupka & Limpus 2005, Bjorndal et al 2005).

The Hawaiian green turtle stock is a recovering stock following severe exploitation for eggs and turtles during the 20th century and has been the subject of extensive nester abundance monitoring (Balazs & Chaloupka 2004a, see Figure 1). This green turtle stock is endemic to the Hawaiian Archipelago and nests mainly on small sand cays in the northwestern Hawaiian Islands region (Balazs & Chaloupka 2004a, Dutton et al 2008).

The multistate capture-mark-recapture modelling approach has been used recently to explore the disease dynamics in terrestrial wildlife such as passerine birds (Faustino et al 2004, Senar & Conroy 2004, Jennelle et al 2007, Conn & Cooch 2009), gopher tortoise (Ozgul et al 2009) and the carnivorous marsupial known as the Tasmanian devil (Lachish et al 2007). This approach to modelling disease dynamics has not been applied to marine wildlife.

## Methods

*Study area and dataset*

The dataset comprised the capture-mark-recapture (CMR) histories for 1904 green turtles from the Hawaiian genetic stock that was sampled over the 29-year period between 1982 and 2010. This specific green turtle foraging ground sample was from Palaau, which is a coastal algae-seagrass habitat on the southside of Molokai (Balazs & Chaloupka 2004b). The Palaau green turtle population has a much higher prevalence of fibropapillomatosis than most other well-studied foraging ground populations that comprise the Hawaiian green turtle genetic stock (Chaloupka & Balazs 2005). Capture and recapture of green turtles from this population was undertaken using a specialized non-selective bullpen net (Balazs & Chaloupka 2004b). Prior to 1996, all turtles were double-marked with uniquely coded Inconel flipper tags but since then the turtles were double-marked with passive integrated transponder tags. There is no evidence of significant tag loss from the Palaau CMR-based program. Details of capture, handling, measurement and tagging methods for this study can be found in Balazs & Chaloupka (2004b). CMR profiles recorded for each turtle included the following — carapace size recorded to the nearest mm as straight carapace length (cm SCL) at first capture and subsequent recaptures using a metal caliper marked in 0.1cm intervals, year of first capture and years-at-large since first capture or previous recapture. There were 816 small immature (< 60cm SCL) and 1088 large immature turtles (≥ 60cm SCL) and no turtles changed sizeclass during the sampling perod. This 2-sizeclass structure was based on the size-specific somatic growth functions derived for various foraging ground populations resident in Hawaiian waters (Balazs & Chaloupka 2004b), which we use to account for potential heterogeneity attributable to size-specific behaviour. Each turtle was also assigned at each encounter to a particular FP disease state based on an ordinal 4-level fibropapilloma tumour severity score (FPS0-3), where 0 = no tumours and 3 = severe affliction (Work & Balazs 1999). The FPS is a readily measured qualitative indicator of

disease severity that correlates with a broad range of pathologic, haematologic and physiologic parameters that reflect deteriorating immunocompetence or health status of Hawaiian green turtles with an increasing tumour affliction (Aguirre & Balazs 2000, Work et al 2003, Chaloupka & Balazs 2005). The disease state was collapsed into a 2-state score as (1) disease-free (FPS=0) and (2) diseased (FPS>1). The dataset then comprised annual CMR histories for 1904 green turtles sampled over a 29-yr period and classified by 2 size-classes and 2 FP disease states (presence/absence).

*Statistical modelling approach*

The MSCMR or multistate extension of the Cormack-Jolly-Seber CMR-based statistical modelling approach (White et al 2006, Jennelle et al 2007) was used to estimate sizeclass- and disease-state-specific survival, recapture and disease-state transition probabilities from the 1904 CMR histories. The MSCMR models were fitted using program MARK (White & Burnham 1999) via the *RMark* package for R (Laake 2013), while model selection was based on the Akaike Information Criterion corrected for sample size (AICc, Burnham & Anderson 2002). MSCMR model assumptions and goodness-of-fit were assessed using the MSCMR-specific metrics proposed by Pradel et al (2005) and implemented in program U-CARE (Choquet et al 2009) as well as the median $\hat{c}$ approach for fitting models by MARK (White et al 2006). A range of MSCMR models were then fitted based on expectations about the disease transmission and recapture processes. Nonlinear functional form in recapture processes was explored using *B*-spline smooths implemented via *RMark* using the *splines* package for R (R Core Team 2014). The best-fit model based on AICc was used to derive the survival, recapture and the disease transmission (infection, recovery) probability estimates. Multimodel inference based on the AICc weights was used to explore the effect of model uncertainty on parameter estimation (Burnham & Anderson 2002), which was also implemented using MARK via *RMark* (Laake 2013). The annual recapture probabilities were used to derive annual Horwitz-Thompson-type population size estimates for diseased and disease-free immature turtles (Bjorndal et al 2005). A precision-weighted smoothing spline regression was then fitted to those estimates to highlight any long-term trend using a generalised smoothing spline regression fitted using the *gss* package for R (Gu 2014) — precision was the inverse of the standard error of the population size estimates. The disease-state-specific annual population size estimates were then used to estimate the annual FP-disease prevalence rate (Chaloupka et al 2009) corrected for imperfect detection with the underlying trend or epidemic curve (and 95% confidence curves) also estimated using a generalised smoothing spline regression (Gu 2014).

**Results**

MSCMR-specific tests of model assumptions and goodness-of-fit suggest an adequate fit overall for the JMV or most general model possible with time-, sizeclass- and disease-state-dependent parameters (JMV: $\chi^2 = 86.21$, df = 119, P = 0.98). There was no evidence of either transient (3G: $\chi^2 = 42.89$, df = 88, P = 0.99) or trap-dependent behaviours (3M: $\chi^2 = 43.32$, df =31, P = 0.08). The variance-inflation factor estimated using U-CARE for the fully time-structured JMV model was $\hat{c} = 0.72$, suggesting slight under-dispersion but many

time-dependent survival and disease-state transition parameters were inestimable due to sparse data and low recapture probabilities (Figure 2).

So a range of reduced-parameter MSCMR models of varying complexity compared to the JMV model were then fitted to the CMR profiles for the 1904 green turtles (Table 1). Transience and trap-dependence were ignored here as well since there was little evidence of these behaviours in the JMV model evaluation. Now the reference model comprised disease-state and sizeclass-specific survival probabilities coupled with state-, sizeclass- and time-specific recapture and disease transition parameters, which is model 35 in Table 1. A number of reduced parameter MSCMR models were found to be far better fits than model 35 with the top five models accounting for ca. 99% of the weight of evidence within this assemble of fitted models (Table 1).

The best-fit model was Model 1, which comprised constant stratum- or disease-state-specific survival probabilities, time-specific recapture probabilities dependent on disease-state, constant sizeclass-specific infection probabilities while the recovery probabilities were also constant but independent of sizeclass. Recapture probabilities were time-dependent but low and this affects robust estimation of many time-dependent parameters (Figure 2). For instance, the data were too sparse to derive robust estimates of time-specific infection or recovery probabilities. In fact, all models with time-dependent disease-state transition probabilities such as Models 37 or 64 were very poor fits compared to Model 1 (Table 1). Moreover, recapture probabilities declined over the 29-yr period and that trend is highlighted in Figure 2 (bottom panel) using a spline-smooth of the recapture parameters in the particular MSCMR model used here for illustrative purposes (in this case recapture parameters were modelled independent of both stratum and sizeclass).

Overall, the best-fit Model 1 accounted for 47% of the weight of evidence (Table 1). The median $\hat{c}$ estimated using MARK for this model was = 1.19 (95% CI: 1.16-1.21), suggesting adequate model fit and no need for using adjusting the model selection metric (AICc) for over-dispersion. Model 2 was very similar to Model 1 differing only in including sizeclass-specific in addition to disease-state-specific survival probabilities — Model 2 accounted for 25% of the weight of evidence (Table 1). Model averaging the survival parameters for the top 5 models in Table 1 results in very similar estimates to the model-specific estimates derived from Model 1.

Disease-state- and sizeclass-specific parameters derived from Model 1 are summarised in Table 2. Disease-state- and/or sizeclass-specific survival probability estimates for Models 1 and 2 are shown in Figure 3, where it is apparent that the parameters were estimated too imprecisely to determine conclusively if there was any sizeclass-specific effect (also compare Model 1 with Model 8). So it was concluded that fibropapilloma (or FP) infection resulted in lower apparent annual survival for immature green turtles resident in Palaau waters, irrespective of sizeclass. The estimated apparent annual survival probability derived from Model 1 for disease-free immature green turtles was 0.882 (95% CI: 0.81-0.93) and 0.779 (95% CI: 0.68-0.85) for FP-diseased immatures. Recapture probabilities were not a function of sizeclass (compare Models 1 and 31) but were both time- and disease-state-dependent, with slightly lower recapture probabilities for FP-diseased immatures (Model 1,

Table). However, irrespective of sizeclass, recapture probabilities were low and there was considerable uncertainty in the precision of those estimates (Figure 2, top panel). The size of the immature green turtle population resident in the Palau sampling area was estimated using the Model 1 recaptures probabilities and it appears that this population has been relatively stable over the 29-yr sampling period with a mean population size ca. 1860 (Figure 4). The estimated proportion or prevalence of FP-diseased turtles in that immature population is shown in Figure 5 with the expected underlying trend since 1983 highlighted using a smoothing spline regression fit.

The estimated annual disease infection rate was not a function of time (compared Models 1 and 37) but there was a sizeclass difference despite considerable uncertainty in parameter estimates with larger turtles having a higher constant probability of infection ca. 0.26 (95% CI: 0.15-0.42) compared to smaller turtles ca. 0.18 (95% CI: 0.11-0.29). The recovery rates derived from the best-fit model (Model 1) were also constant (time-independent) but with little meaningful difference between small immature turtles (0.16, 95% CI: 0.07-0.34) and the larger immature turtles (0.145, 95% CI: 0.07-0.29). The rates of disease transmission (infection, recovery) may well be time-dependent for this green sea turtle population, but the low recapture probabilities were far too low to be able to estimate such models with any precision. Such models were poor relative fits to the CMR dataset with little if any weight of evidence in support of such models in this ensemble (see Models 37 and 64 in Table 1). The time-dependent disease transmission model fits such as Models 37 and 64 comprised many inestimable parameters for the infection rate but the few estimable rates that could be gleaned from Model 37 have been included in Figure 5 to show the comparison with the prevalence estimates derived from the disease-state-dependent abundance estimates.

**Discussion**

The green sea turtle is the most abundant marine megaherbivore with major nesting populations either stable or increasing in abundance following intensive conservation actions over the past few decades (Chaloupka et al 2008a). The Hawaiian green turtle nester population is also increasing (Figure1) following protection from exposure to various anthropogenic hazards such as harvesting and habitat destruction (Balazs & Chaloupka 2004a, Chaloupka & Balazs 2007).

However, reliable estimates of key demographic parameters such as mortality and recruitment are needed for modelling the risk of marine turtle population exposure to anthropogenic hazards (Chaloupka 2003) and for diagnosing any trends in population abundance (Bjorndal et al 2011). But deriving such estimates for long-lived marine species such as green turtles that live in vast oceanic and neritic habitats is a major challenge.

The disease-free constant annual survival probability estimate for immatures is consistent with estimates for other green turtle populations (Chaloupka et al. 2005). Similar estimates of survival probability as for the Bahamas green stock (Bjorndal et al 2003) and the southern Great Barrier Reef green turtle stock Chaloupka 2004).

Recapture probabilities were time-varying but were independent of either disease state or sizeclass (Table 2), which suggests that there was no sampling bias or behavioral differences for the diseased turtles and so that a simple apparent prevalence curve would not be biased for this study (see Senar & Conroy 2004, Jennelle et al. 2007). The estimated disease state transition probabilities suggested a rapidly increasing infection rate following the disease outbreak in the early-1980s followed by a significant and gradual decline from the mid-1990s as the disease ran its course (Table 2). This infection rate function reflected well the apparent FP disease prevalence curve estimated for this population (see Fig. 1c in Chaloupka et al. in review). At the peak of the epidemic in the mid-1990s (piecewise interval years 10-14, Table 2) it was estimated that the infection probability was > 0.43 (95% CI: 0.29-0.58). The current annual infection rate has declined to ca. 0.032 (piecewise interval years 19-23, Table 2).

**References**


Aguirre A, Balazs G (2000) Blood biochemistry values of green turtles, *Chelonia mydas*, with and without fibropapillomatosis. Comparative Haematology International 10: 132-137

Balazs G, Chaloupka M (2004a) Thirty-year recovery trend in the once depleted Hawaiian green sea turtle stock. Biological Conservation117: 491-498

Balazs G, Chaloupka M (2004b) Spatial and temporal variability in somatic growth of green sea turtles resident within the Hawaiian Archipelago. Marine Biology 145: 1043-1059

Bjorndal K, Bolten A, Chaloupka M (2003) Survival probability estimates for immature green turtles *Chelonia mydas* in the Bahamas. Marine Ecology Progress Series 252: 273-281

Bjorndal K, Bolten A, Chaloupka M (2005) Evaluating trends in abundance of immature green turtles, *Chelonia myas*, in the greater Caribbean. Ecological Applications 15: 304-314

Bjorndal K, Bowen B, Chaloupka M, Crowder L, Heppell S, Jones C, Lutcavage M, Policansky D, Solow A, Witherington B (2011) Better science needed for restoration in the Gulf o fMexico. Science 331: 537-538

Burnham K, Anderson D (2002) Model selection and multi-model inference: a practical information-theoretic approach. Second edn. Springer-Verlag, New York, USA

Chaloupka M (2003) Stochastic simulation modelling of loggerhead sea turtle population dynamics given exposure to competing mortality risks in the western south Pacific. p 274-294, In: Bolten AB, Witherington B (Eds) Loggerhead Sea Turtles. Smithsonian Institution Press, Washington, DC, USA

Chaloupka M (2004) Exploring the metapopulation dynamics of the southern Great Barrier

Reef green turtle stock and possible consequences of sex-biased local harvesting. In: Akçakaya H, Burgman M, Kindvall O, Wood C, Sjogren-Gulve P, Hattfield J, McCarthy M (eds) Species conservation and management: case studies. Oxford University Press, New York, p 340-354

Chaloupka M, Balazs G (2005) Modelling the effect of fibropapilloma disease on the somatic growth dynamics of Hawaiian green sea turtles. Marin Biology147: 1251-1260

Chaloupka M, Balazs, G (2007) Using Bayesian state-space modelling to assess the recovery and harvest potential of the Hawaiian green sea turtle stock. Ecological Modelling 205: 93-109

Chaloupka M, Balazs G, Work T (2009) Rise and fall over 26 years of a marine epizootic in Hawaiian green sea turtles. Journal of Wildlife Diseases 45: 1138-1142

Chaloupka M, Bjorndal K, Balazs G, Bolten A, Ehrhart L, Limpus C, Suganuma H, Troëng S, Yamaguchi M (2008a) Encouraging outlook for recovery of a once severely exploited marine megaherbivore. Global Ecology and Biogeography 17: 297-304

Chaloupka M, Limpus C (2005) Estimates of sex- and age-class-specific survival probabilities for a southern Great Barrier Reef green sea turtle population. Marine Biology 146: 1251-1261

Chaloupka M, Work T, Balazs G, Murakawa S, Morris R (2008) Cause-specific temporal and spatial trends in green sea turtle strandings in the Hawaiian Archipelago (1982-2003). Marine Biology 154: 887-898

Choquet R, Lebreton J, Gimenez O, Reboulet A, Pradel R (2009) U-CARE: Utilities for performing goodness of fit tests and manipulating CApture-Recapture data. Ecography 32: 1071–1074

Conn P, Cooch E (2009) Multistate capture-recapture analysis under imperfect state observation: an application to disease models. Journal of Animal Ecology 46: 486-492

Cooch E, Conn P, Ellner S, Dobson A, Pollock K (2010) Disease dynamics in wild poulations: modeling and estimation: a review. Journal of Ornithology 152 (Supplement 2): S485-509

Dutton P, Balazs G, LeRoux R, Murakawa S, Zárate P, Sarti Martínez L (2008) Composition of Hawaiian green turtle foraging aggregations: mtDNA evidence for a distinct regional population. Endangered Species Research 5: 37–44

Faustino C, Jennelle C, Connolly V, Davis A, Swarthout E, Dhondt A, Cooch E (2004) *Mycoplasmagallisepticum* infection dynamics in a house finch population: seasonal variation in survival, encounter and transmission rate. Journal of Animal Ecology 73: 651–669

Gu C (2014) Smoothing spline ANOVA models: R package gss. Journal of Statistical Software 58(5): 1-25

Jennelle C, Cooch E, Conroy M, Senar J (2007) State-specific detection probabilities and disease prevalence. Ecological Applications17: 154-167

Laake J (2013) RMark: An R interface for analysis of capture-recapture data with MARK. AFSC Processed Rep 2013-01, 25p. Alaska Fisheries Science Centre, National Marine Fisheries Service, 7600 Sand Point Way NE, Seattle

Lachish S, Jones M, McCallum H (2007) The impact of disease on the survival and population growth rate of the Tasmanian devil. Journal of Animal Ecology 76: 926-936

Pradel R, Gimenez O, Lebreton J (2005) Principles and interest of GOF tests for multistate capture-recapture models. Animal Biodiversity and Conservation 28: 189-204

R Core Team (2014) R: A language and environment for statistical computing. R Foundation for Statistical Computing, Vienna, Austria. http://www.R-project.org/

Senar J, Conroy M (2004) Multi-state analysis of the impacts of avian pox on a population of Serins (*Serinus serinus*): importance of estimating recapture rates. Animal Biodiversity and Conservation 27: 133-146

Troëng S, Chaloupka M (2007) Variation in adult annual survival probability and remigration intervals of seaturtles. Marine Biology151: 1721–1730

White G, Burnham K (1999) Program MARK: survival estimation from populations of marked animals. Bird Study 46 (Supplement): 120-138

White G, Kendall W, Barker R (2006) Multistate survival models and their extension in Program MARK. Journal of Wildlife Management 70: 1521-1529

Work T, Balazs G (1999) Relating tumor score to hematology in green turtles with fibropapillomatosis in Hawaii. Journal of Wildlife Diseases 35: 804-807

Work T, Balazs G, Wolcott M, Morris R (2003) Bacteraemia in free-ranging Hawaiian green turtles *Chelonia mydas* with fibropapillomatosis. Diseases in Aquatic Organisms 53: 41-46

**Table1** CMR multistate model summary for sizeclass- and stratum (disease-state)-dependent survival, recapture, transmission rates (infection, recovery). np=number of estimable parameters, AICc = sample size corrected Akaike Information Criterion, ΔAICc = change in AICc from previous model, weight = model weight in favour of that model in the model assemble summarised in the table, dev=deviance, time = sampling occasion (categorical), Time = sampling occasion (ordinal), bs(Time,6) = B-spline smooth of sampling occasion with degrees of freedom = 6. 2 sizeclasses = size (small immatures, large immatures). 2 diseases states = stratum (FP disease free, FP diseased). Top 5 models account for 99% of the weight of evidence in the model set.

| # | survival ($\phi$) | recapture ($\rho$) | disease-state transitions ($\psi$) | np | AICc | ΔAICc | weight | dev |
|---|---|---|---|---|---|---|---|---|
| 1 | ~stratum | ~stratum*time | ~ -1+stratum:tostratum:size | 54 | 3276.52 | 0.00 | 0.473 | 995.17 |
| 2 | ~stratum*size | ~stratum*time | ~ -1+stratum:tostratum:size | 56 | 3277.83 | 1.31 | 0.246 | 992.27 |
| 3 | ~stratum | ~stratum*time | ~ size+stratum:tostratum:size | 55 | 3278.63 | 2.10 | 0.165 | 995.17 |
| 4 | ~stratum*size | ~stratum*time | ~ size+stratum:tostratum:size | 57 | 3279.94 | 3.42 | 0.086 | 992.27 |
| 5 | ~stratum | ~stratum*time | ~ size:stratum+size:tostratum | 57 | 3282.85 | 6.32 | 0.020 | 995.17 |
| … | | | | | | | | |
| 8 | ~size | ~stratum*time | ~ -1+stratum:tostratum:size | 54 | 3297.83 | 21.30 | 0.000 | 1016.48 |
| 23 | ~stratum*size | ~size*time | ~ -1+stratum:tostratum:size | 56 | 3324.19 | 47.67 | 0.000 | 1038.63 |
| 31 | ~stratum | ~stratum*size*time | ~ -1+stratum:tostratum:size | 102 | 3334.64 | 58.11 | 0.000 | 949.82 |
| 35 | ~stratum*size | ~stratum*size*time | ~-1+stratum:tostratum:size | 104 | 3345.09 | 68.56 | 0.000 | 955.85 |
| 37 | ~size | ~stage*time | ~ -1+stratum:tostratum:time | 106 | 3352.74 | 76.22 | 0.000 | 959.08 |
| 38 | ~size | ~stratum*size*time | ~ -1+stratum:tostratum:size | 102 | 3353.83 | 77.31 | 0.000 | 969.01 |
| … | | | | | | | | |
| 43 | ~stratum | ~size*bs(Time, 6) | ~ -1+stratum:tostratum:size | 20 | 3358.24 | 81.72 | 0.000 | 1147.35 |
| 44 | ~size | ~size*bs(Time, 6) | ~ -1+stratum:tostratum:size | 20 | 3358.79 | 82.27 | 0.000 | 1147.90 |
| 64 | ~size | ~size*bs(Time, 6) | ~ -1+stratum:tostratum:time | 72 | 3386.79 | 110.27 | 0.000 | 1067.20 |

**Table2** Summary of best-fit multistate model parameters (see model 1 in Table1)

| parameter | estimate | se | lower CI | upper CI |
|---|---|---|---|---|
| *survival probabilities (disease-state dependent)* | | | | |
| disease-free immatures | 0.8821 | 0.0292 | 0.8117 | 0.9285 |
| diseased immatures | 0.7794 | 0.0419 | 0.6867 | 0.8507 |
| *infection rates (time period independent, sizeclass-specific)* | | | | |
| small immatures | 0.180 | 0.048 | 0.105 | 0.293 |
| large immatures | 0.260 | 0.069 | 0.149 | 0.415 |
| *recovery rates (time period independent, sizeclass-specific)* | | | | |
| small immatures | 0.160 | 0.067 | 0.067 | 0.337 |
| large immatures | 0.145 | 0.056 | 0.066 | 0.289 |

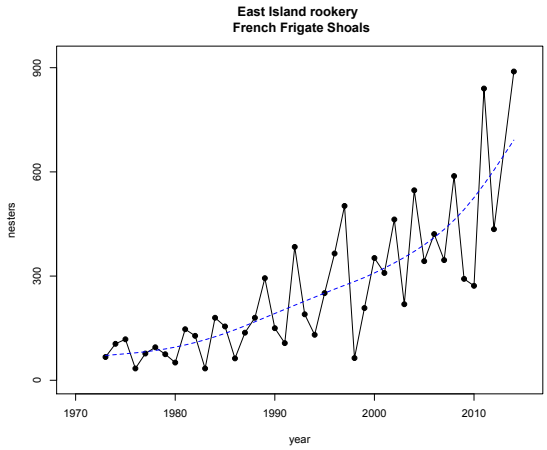


**Figure 1** Estimated green turtle nester abundance since 1973at East Island (French Frigate Shoals, Hawaii). Solid dots show the annual population size estimates, dashed curve is a smoothing spline highlighting any underlying trend.

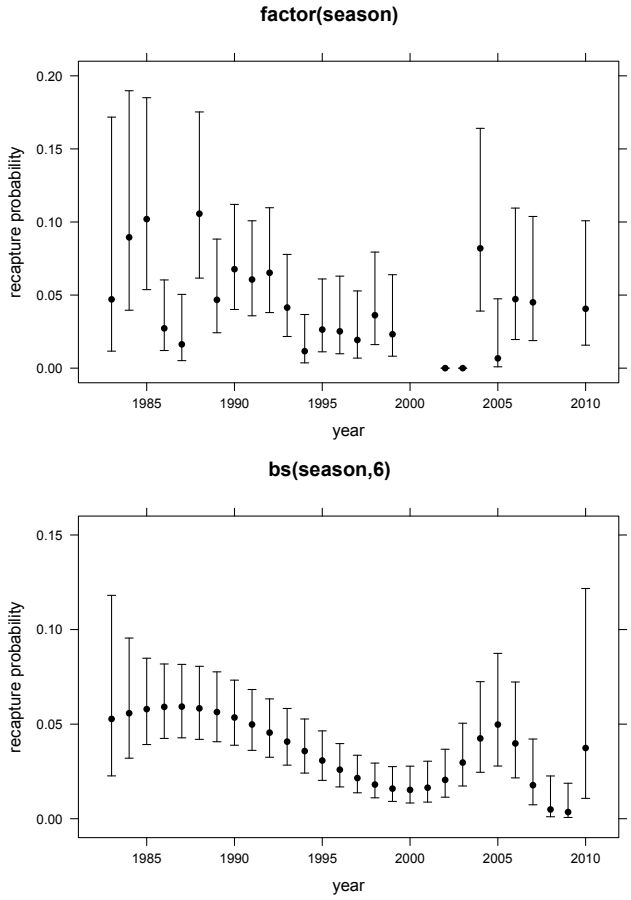


**Figure 2** Estimated green turtle nester abundance since 1973at East Island (French Frigate Shoals, Hawaii). Solid dots show the annual population size estimates, dashed curve is a smoothing spline highlighting any underlying tren

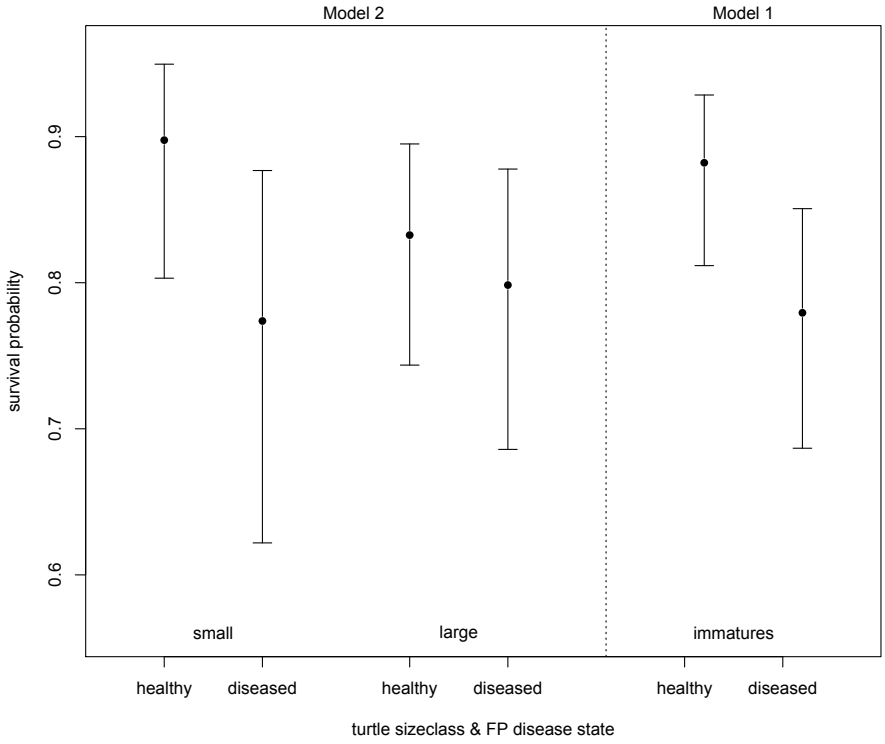


**Figure 3** Estimated green turtle nester abundance since 1973at East Island (French Frigate Shoals, Hawaii). Solid dots show the annual population size estimates, dashed curve is a smoothing spline highlighting any underlying trend.

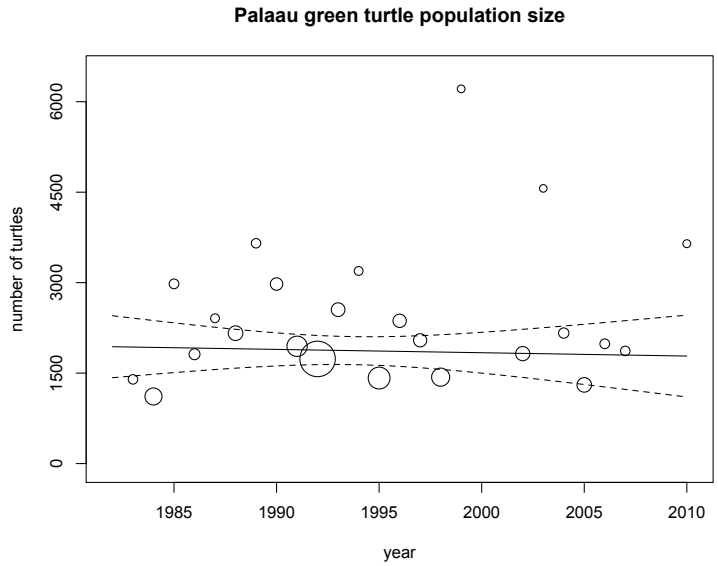


**Figure 4** Estimated immature green turtle abundance (disease free and FP-diseased turtles) since 1983 at the Palau foraging ground (Molokai, Hawaii). Open dots show population size estimates, dot size proportional to variance of each estimate, solid curve is a smoothing spline regression fit to highlight any underlying trend, dashed curves = 95% Bayesian confidence curves

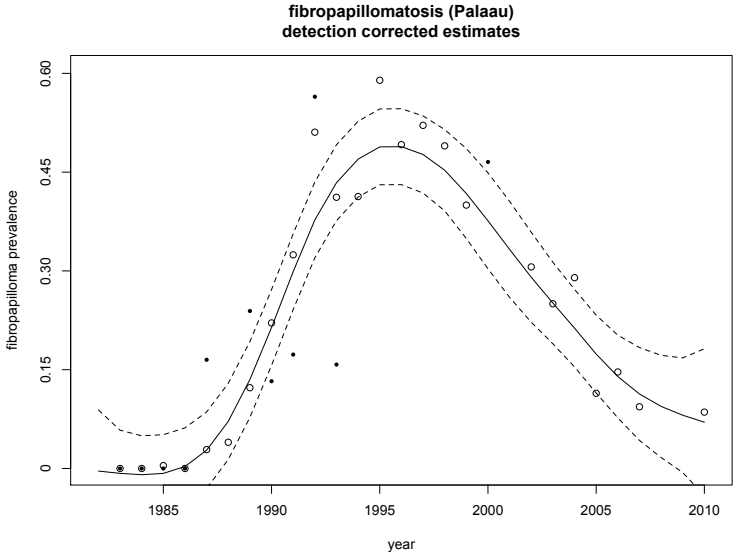


**Figure 5** Epidemic or prevalence curve derived from the detection-corrected disease-state-dependent population size estimates. Solid curve = smoothing spline regression fit, dashed curves = 95% Bayesian confidence curves, open dots = apparent prevalence estimates, solid dots = infection rate estimates from Model 37 (Table 1).